Taylor & Francis
Taylor & Francis Group

ORIGINAL RESEARCH

🔓 OPEN ACCESS   ⟳ Check for updates

Sustained localized delivery of immunotherapy to lymph nodes reverses immunosuppression and increases long-term survival in murine glioblastoma

John Choi[a], Ayush Pant[a]*, Ravi Medikonda[a], Young-Hoon Kim[b], Denis Routkevitch[a], Laura Saleh[a], Luqing Tong[a], Hok Yee Chan[a], Jessie Nedrow[c], Christopher Jackson[a], Christina Jackson[a], and Michael Lim 🆔[a]

[a]Department of Neurosurgery, Johns Hopkins School of Medicine, Johns Hopkins University, Baltimore, USA; [b]Department of Neurosurgery, College of Medicine, Asan Medical Center, University of Ulsan, Songpa-gu, Seoul, Republic of Korea; [c]Department of Radiology, Radiological Physics Division, Johns Hopkins School of Medicine, Johns Hopkins University, Baltimore, USA

ABSTRACT

Introduction: Despite the advent of immunotherapy as a promising therapeutic, glioblastoma (GBM) remains resistant to using checkpoint blockade due to its highly immunosuppressive tumor milieu. Moreover, current anti-PD-1 treatment requires multiple infusions with adverse systemic effects. Therefore, we used a PCL:PEG:PCL polymer gel loaded with anti-PD-1 and implanted at the site of lymph nodes in an attempt to maximize targeting of inactivated T cells as well as mitigate unnecessary systemic exposure.

Methods: Mice orthotopically implanted with GL261 glioma cells were injected with hydrogels loaded with anti-PD-1 in one of the following locations: cervical lymph nodes, inguinal lymph nodes, and the tumor site. Mice treated systemically with anti-PD-1 were used as comparative controls. Kaplan–Meier curves were generated for all arms, with ex vivo flow cytometric staining for L/D, CD45, CD3, CD4, CD8, TNF-α and IFN-y and co-culture ELISpots were done for immune cell activation assays.

Results: Mice implanted with PCL:PEG:PCL hydrogels carrying anti-PD-1 at the site of their lymph nodes showed significantly improved survival outcomes compared to mice systemically treated with anti-PD-1 ($P = .0185$). Flow cytometric analysis of brain tissue and co-culture of lymph node T cells from mice implanted with gels demonstrated increased levels of IFN-y and TNF-α compared to mice treated with systemic anti-PD-1, indicating greater reversal of immunosuppression compared to systemic treatment.

Conclusions: Our data demonstrate proof of principle for using localized therapy that targets lymph nodes for GBM. We propose an alternative treatment paradigm for developing new sustained local treatments with immunotherapy that are able to eliminate the need for multiple systemic infusions and their off-target effects.

Introduction

Immunotherapy has revolutionized the treatment of cancers across multiple subtypes.[1–4] The use of immune checkpoint blockade (ICB) – most notably directed at Programmed Cell Death Protein-1 receptor (PD-1) and cytotoxic T-lymphocyte-associated protein 4 (CTLA-4) – rejuvenate anti-tumor responses in inactivated T cells and demonstrate great promise in treating tumors such as melanoma and non-small cell lung cancer.[5–7] Despite the success of ICB therapy in these cancers, however, glioblastoma (GBM) remains resistant to current immunotherapeutic strategies due to its immunosuppressive milieu preventing rescue of inactivated T cells and myeloid cells[8].

Additionally, current anti-PD-1 therapy is dose-limited by immune-related adverse events (irAEs). Despite the synergistic therapeutic benefit of targeting multiple checkpoint molecules for GBM[9], irAEs such as nephritis and pruritus are especially pronounced in combination immunotherapy, with several other documented sequelae such as pneumonitis, colitis, vitiligo, and hypophysitis seen as consequences of checkpoint

blockade[10]. This is particularly an issue for GBM as anti-PD-1 monotherapy alone is unlikely to offer sufficient therapeutic benefit[11].

Enhancing localized, tumor-targeting immunotherapy would be an important leap forward in cancer immunotherapy that would reduce off-target toxicities while increasing drug efficacy to allow for higher doses of ICB or combination therapy. Many modalities have been tested to achieve this goal, from using irradiated tumor cells to secrete monoclonal antibodies against CTLA-4 at the immunization site to intratumoral injection of adoptively transferred immune cells such as dendritic cells[12].

Our current study examines the potential of targeting lymph nodes – sites of antigen presentation and cytotoxic immune cell activation – using hydrogels that can offer sustained, localized delivery of antibodies such as anti-PD-1. Since our targets are inactivated T cells, the tumor-draining lymph nodes act as an optimal alternative to targeting the tumor itself; as the site of T cell activation with robust trafficking of professional antigen presenting

CONTACT John Choi ✉ jchoi134@stanford.edu 🖳 Department of Neurosurgery, Johns Hopkins School of Medicine, Johns Hopkins University, Baltimore 21231, USA
*These authors contributed equally to this work.

cells, there is a high likelihood of interacting with immune cells that have the potential for re-activation and expansion of anti-tumor phenotypes, moreover, as a hub of multiple immune cells including myeloid cells, lymph node exposure to immunotherapeutic agents such as anti-PD-1 into the lymph nodes would also target additional cell types that might benefit from checkpoint blockade[13–16]. Through this investigation, we explored the novel strategy of using sustained localized delivery of anti-PD-1 to lymph nodes in a murine preclinical model, providing survival data and immunophenotype analysis of its benefits over systemic therapy.

Materials and methods

Murine glioma model and cell lines

Female 6–8 week-old C57BL/6 J wild-type mice were maintained at the Johns Hopkins University Animal Facility per the Institutional Animal Care and Use Committee (IACUC) protocol. For all *in vivo* experiments, mice were anesthetized with Ketathesia (100 mg/kg)/xylazine (10 mg/kg) via intra-peritoneal (i.p.) injection and had topical eye gel for lubrication while anesthetized. Mice were placed on a heating pad and observed until fully recovered. GL261-Luc2 cells grown in DMEM (Life Technologies) + 10% FBS (Sigma-Aldrich) + 1% penicillin-streptomycin (Life Technologies) were used for orthotopic murine glioma models, as described in previous studies[17]. 1.3e5 GL261-Luc2 cells in a volume of 2 uL were stereotactically injected 2 mm lateral to the sagittal suture, 2 mm posterior to the coronal suture, and 3 mm deep to the cortical surface in the area of the left striatum. After implantation of tumor cells, mice were assessed for tumor growth on post-implantation day 7 using bioluminescent IVIS® imaging (PerkinElmer).

Mice with sufficient tumor burden at day 7 were then randomly separated into control (non-treated) and treatment arms. The presence of tumor was then monitored by IVIS® imaging on post-implantation days 14, 21, 28, and 40. Survival experiments were repeated in triplicate with 8–10 mice in each control or treatment arm. Animals were euthanized according to humane endpoints, including CNS disturbances, hunched posture, lethargy, weight loss, and inability to ambulate per our IACUC protocol.

Flank tumor models involved female 6–8 week-old C57BL/6 J wild-type mice that were subcutaneously injected in the left hind limb with 10^6 GL262 cells in 100 uL of mixed PBS and Matrigel (BD Biosciences) in a 1:1 ratio. Mice were treated either intra-peritoneally with anti-PD-1 on days 10, 12, and 14, or implanted with hydrogel loaded-anti-PD-1 (see below in "Therapeutic antibodies") on day 10 at region of the left inguinal lymph node. Control mice were not treated with anti-PD-1. Tumor growth was measured every 2 days using calipers and tumor volumes were calculated in three dimensions using the formula: $4/3\pi r.^3$

Therapeutic antibodies

G4 hybridomas were cultured and used to develop hamster monoclonal antibodies (mAbs) against murine PD-1, as described in previous studies[18]. Therapeutic murine antibodies were subsequently stored in 1 mg/mL and 3 mg/mL aliquots at −80°C. To concentrate anti-PD-1 for hydrogel mixtures, 15 mL AMICON ultrafiltration tubes were used to concentrate anti-PD-1 into 100 ug/ul solutions (MilliporeSigma), with concentrations determined by Nanodrop (Wilmington, DE, USA).

Individual treatment dose was 200 ug per dose on post-implantation days 10, 12, and 14 for anti-PD-1 i.p. injections and 600 ug total for PCL:PEG:PCL hydrogel implantations. Mice implanted with hydrogels loaded with anti-PD-1 were given 50 ul of hydrogel carrying 600 ug anti-PD-1. Hydrogels were implanted <3 mm superficial to the inguinal and deep cervical lymph nodes in the left groin and neck, respectively.

Reconstitution of Hydrogel

The PCL:PEG:PCL hydrogel was generously provided to the laboratory of Dr Michael Lim by BTG plc. The aqueous solution of the hydrogel was stored at −20°C and left at room temperature (25°C) overnight. Aliquots were heated in a 60°C water bath for 20 minutes with intermittent vigorous shaking (every 2 minutes). Afterward, the bottle was left to stand at 25°C for 3 hours and then transferred to 4°C for 2 hours. At this point, the polymer was a clear liquid that was mixed with the appropriate concentration of PD-1 antibody to create 50 uL aliquots of the gel. All aliquots were stored on ice and filtered through a .22um syringe filter.

Immune cell harvest and isolation

Mice were deeply anesthetized or euthanized before harvesting lymph nodes or brains for immunological assays per our IACUC protocol. Red blood cells in brain and lymph node samples were lysed using ACK lysis buffer (ThermoFisher) and resuspended in phosphate buffered saline (PBS) buffer for further cytometric staining. Brains were removed, tissue was mechanically dissociated through a 70 um filter, and homogenates were centrifuged in a 30%/70% Percoll® (Sigma-Aldrich) gradient at 2200 rpm for 20 minutes without brakes to separate out brain myeloid cells and lymphocytes from tumor cells and myelin. Brain immune cells were extracted at the 30%/70% interface and resuspended in PBS buffer (Sigma-Aldrich) for further cytometric analysis. Lymph nodes were mechanically dissociated through a 70 um filter, centrifuged at 300 g, and washed in PBS buffer for further cytometric staining and analysis.

Flow cytometric analysis of murine immune cells

Mouse immune cells were stained for Live/Dead (L/D) (Invitrogen), CD45, CD3, CD4, CD8, IFN-γ, and TNF-α (Figure 3). To stain for the intracellular marker IFN-γ and TNF-α, samples were fixed in 1:3 fixation/permeabilization concentrate: diluent mixture (eBioscence) for 30 minutes and subsequently stained in permeabilization buffer (eBioscence).

Fluorescence minus one (FMO) was used to control for data spread due to multiple fluorochromes and nonbinary expression of markers such as IFN-γ and TNF-α. Flow data were acquired using a FACSCelesta flow cytometer (BD) and analyzed using FlowJo (BD). Nonviable cells and doublets were excluded by forward versus side scatter gating, forward scatter height versus forward scatter area gating, and L/D staining.

Radiolabeling and radiotracking harvest experiments

Using previously described methods, the anti-PD-1 antibody was conjugated to N-[2-amino-3-(p-isothiocyanatophenyl) propyl]-trans-cyclohexane-1,2-diamine-N,N',N',N'',N''-pentaacetic acid (SCN-CHX-A″-DTPA) with Indium[111] added to an acid washed solution containing antibody[19][20]. The mixture was set at 25°C for 1 h and then transferred to an Amicon Ultrafiltration device with the protein concentration determined by Nanodrop (Wilmington, DE, USA). A 200 ug of the conjugated anti-PD-1 antibody was mixed with the hydrogel in a 1:3 ratio and implanted into the left inguinal or anterior cervical regions of mice. On days 1 and 9, mice were harvested for their blood, liver, spleen, kidney, bone, deep cervical lymph nodes, inguinal lymph nodes, and brain and measured by weight and gamma well counter using a 400 to 480 keV energy window (PerkinElmer 2470 WIZARD2® Automatic Gamma Counter, MA, USA). The percent-injected activity per gram (%IA/g) was calculated by comparison to a weighted, diluted standard.

Co-culture and ELISpot

For IFN-γ assays, 5e3 CD45.2+ CD3 + T cells were sorted from either inguinal or deep cervical lymph nodes in tumor-bearing mice on post-implantation day 14 that received no treatment, treatment with i.p. injected anti-PD-1, treatment with hydrogels at the inguinal lymph node, or treatment with hydrogels adjacent to the deep cervical lymph nodes. These T cells were co-cultured with 100 ug/ml GL261-Luc2 tumor cell lysate and 25e3 dendritic cells isolated from CD45.1 mouse spleen (isolated with a pan-dendritic cell isolation kit) (Miltenyi Biotec) in a 96-well round bottomed plate with T cell media (RPMI 1640 + 10% FBS + 1% NEAA + 1% 2-Mercaptoethanol + 1% Penicillin/Streptomycin). Co-cultured cells were incubated at 37°C for 48 hours. Supernatant was collected for subsequent ELISA for IFN-γ and run on a plate reader (Thermo Fisher).

Statistical analysis

All replicates were biological replicates. Survival was analyzed via Kaplan–Meier method and compared by log-rank (Mantel-Cox) test. Calculated variables were treated as continuous variables under the assumption that data follow Student T-distribution. Mouse experimental data were analyzed using a two-tailed Student's T-test for experiments containing two groups. Comparisons between groups were presented as mean ± SEM. All data were analyzed using GraphPad Prism 8 and values of $P < .05$ were considered statistically significant.

Results

Hydrogel-mediated release of anti-PD-1 results in sustained delivery of antibody to nearby lymph nodes and to glioblastoma

To evaluate whether the PCL:PEG:PCL hydrogel could facilitate sustained delivery of anti-PD-1 antibody to lymph nodes *in vivo*, mice were injected with hydrogels loaded with ^{111}In-DTPA-anti-PD-1 in their inguinal and anterior cervical regions in both the absence (Figure 1) and presence (Figure 2) of tumor. The physical integrity of the hydrogel remained intact for the duration of the 9 days between initial and final organ harvests for detecting anti-PD-1 (Figure 1a).

Non-tumor-bearing mice injected with loaded hydrogels in the inguinal region demonstrated localization of anti-PD-1 to
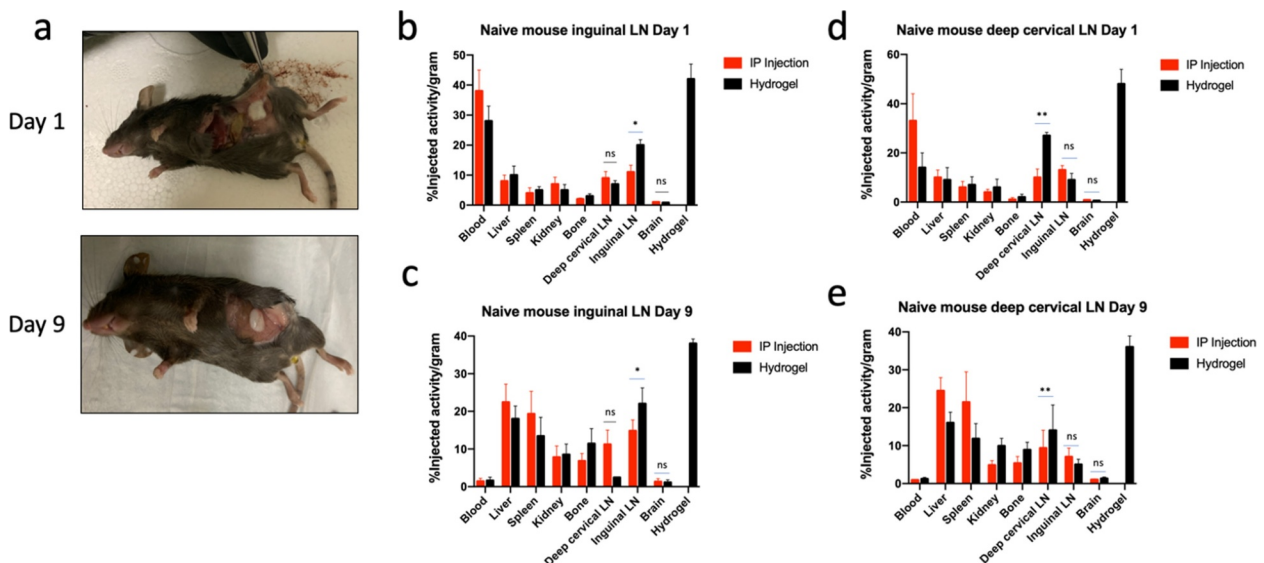
Figure 1. Hydrogel-mediated release of anti-PD-1 has sustained deposition into local lymph nodes. (a) Day 1 and 9 mouse harvests demonstrating intact presence of hydrogel at the site of the left inguinal lymph node. (b,c) Day 1 and 9 of organ harvests in non-tumor-bearing mice that have been implanted with hydrogels loaded with anti-PD-1 at the site of the left inguinal region (n = 3 per arm). (d,e) Day 1 and 9 of organ harvests in non-tumor-bearing mice that have been implanted with hydrogels loaded with anti-PD-1 at the site of the left anterior cervical region (n = 3 per arm). (** $P < .01$, * $P < .05$).
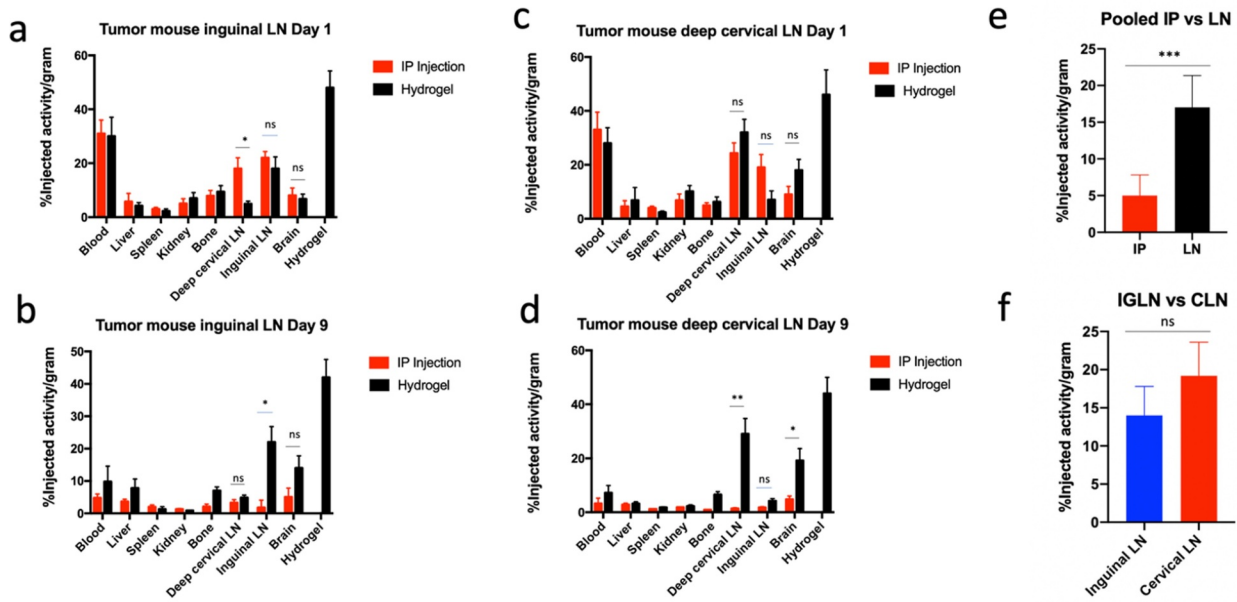
Figure 2. Glioma-bearing mice exhibit different distribution of anti-PD-1 in the brain depending on delivery mechanism of anti-PD-1. (a,b) Day 1 and 9 of organ harvests in GL261-bearing mice that have been implanted with hydrogels loaded with anti-PD-1 at the site of the left inguinal region (n = 3 per arm). (c,d) Day 1 and 9 of organ harvests in GL261-bearing mice that have been implanted with hydrogels loaded with anti-PD-1 at the site of the left anterior cervical region (n = 3 per arm). (e) Comparison between pooled i.p. injection and hydrogel treated mice for anti-PD-1 distribution in the brain (pooled n = 6 per arm). (f) Comparison between inguinal lymph node and cervical lymph node treated mice for anti-PD-1 distribution in the brain (n = 3 per arm) (** P < .01, * P < .05).

the inguinal lymph nodes when compared to i.p. injection on both day 1 (P = .0369) and day 9 (P = .0316) post-injection (Figure 1bc). There was no significant difference in percent-injected activity per gram (%IA/g) in the cervical lymph nodes for administration of anti-PD-1 through i.p. or inguinal hydrogel routes (Figure 1bc). Within the non-tumor-bearing mice that were injected at the anterior cervical site, %IA/g was significantly higher in the deep cervical lymph nodes for mice that had cervical hydrogel placement compared to i.p. delivery on both day 1 (P = .0095) and day 9 (P = .0021). Of note, there were no significant differences in the %IA/g of anti-PD-1 in the brain from i.p. vs hydrogel-based delivery for any of the non-tumor-bearing groups (Figure 1b-d).

Similarly, mice bearing intracranial glioma demonstrated sustained delivery of anti-PD-1 to their local lymph nodes (Figure 2). Interestingly, glioma-bearing mice implanted with hydrogel in the inguinal region on day 1 had lower concentrations of anti-PD-1 in their deep cervical lymph nodes (Figure 2a) than those mice given i.p. anti-PD-1. Otherwise, there were no significant differences between anti-PD-1 distribution from i.p. and hydrogel delivery routes on day 1 (Figure 2ac). On day 9, sustained delivery to nearby lymph nodes was noted for tumor-bearing mice with hydrogel injected; mice with hydrogel at their inguinal region had significantly greater %IA/g of anti-PD-1 in their inguinal lymph nodes, while the deep cervical lymph nodes showed comparable levels of %IA/g between i.p. and hydrogel arms (Figure 2b). In a similar manner, tumor-bearing mice with injection of hydrogel in the anterior cervical region demonstrated increased representation of anti-PD-1 in the deep cervical lymph nodes, but minimal activity in the inguinal lymph nodes (Figure 2d). Of note, tumor-bearing mice with hydrogel in the cervical region had a significantly different level of anti-

PD-1 in the brain on day 9 when compared to mice treated with anti-PD-1 (Figure 2d).

Although the increase in anti-PD-1 levels in the brain of inguinal hydrogel-treated mice compared to i.p. treated mice was not statistically significant in Figure 2b, pooling i.p. treated mice with brain tumors from Figure 2b and Figure 2d (both harvested day 9 after i.p. injection) shows a statistically significant difference in anti-PD-1 levels in brain between i.p. injection and lymph node implantation (P = .0002, Figure 2e). In addition, the %IA/g of anti-PD-1 in the brain of inguinal hydrogel-injected mice was not significantly different from that of cervical hydrogel-injected mice, suggesting that sustained anti-PD-1 delivered locally to lymph nodes eventually accumulates in brain tumors regardless of the target lymph node (P = .1641, Figure 2f).

Notably, the %IA/g of anti-PD-1 nine days after i.p. treatment is diminished in multiple tissues including kidneys, spleen, liver and bones of tumor-bearing mice compared to healthy counterparts, possibly due to the systemic immuno-suppressive effect of intracranial tumors that result in a dearth of circulating lymphocyte populations that are able to bind the anti-PD-120. Despite the systemic immunosuppressive response in glioma-bearing mice, injecting hydrogel and anti-PD-1 admixture in the lymph nodes allowed focused delivery of anti-PD-1 to the site of anti-tumor priming (lymph nodes) and anti-tumor activity (brain), allowing amelioration of immune response.

Lymph nodes exposed to sustained anti-PD-1 show increased immunogenic activity compared to those exposed to systemic anti-PD-1

In order to assess the immunogenic potential of anti-PD-1 checkpoint blockade in a GBM model, mice were administered with either i.p. (systemic) therapeutic anti-PD-1 or hydrogel-
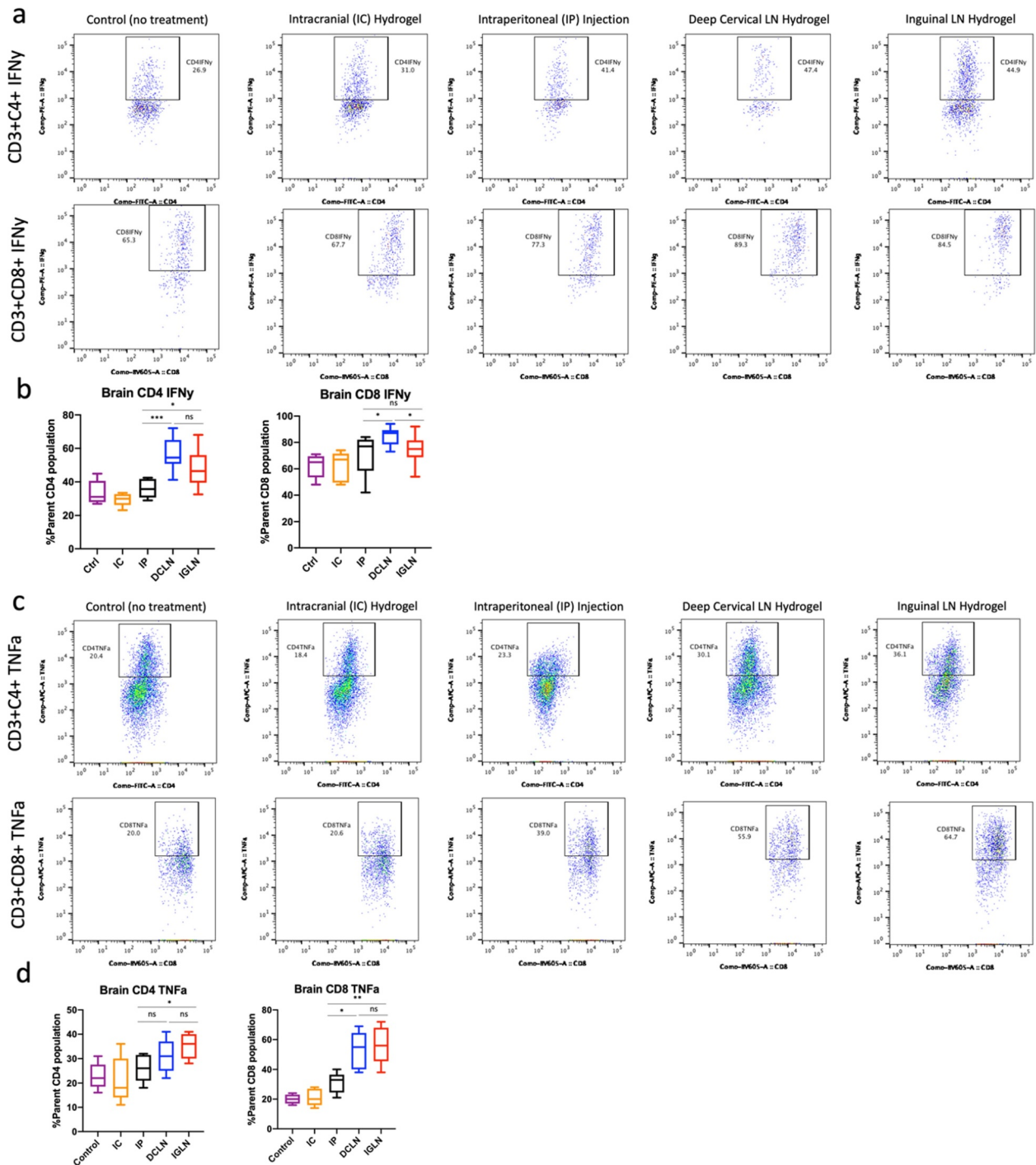
Figure 3. Flow cytometric analysis of harvested tumor-bearing mouse brain with polymer-based vs systemic vs intracranial delivery of anti-PD-1. Mice were either not treated or given intracranial hydrogel (loaded with 200 ug anti-PD-1), intraperitoneal injection of anti-PD-1 (total dose 600 ug spaced over five days), cervical hydrogel (loaded with 600 ug of anti-PD-1), and inguinal hydrogel (loaded with 600 ug of anti-PD-1). (a) Flow cytometry plots demonstrating %parent populations of CD4+ and CD8+ IFN-γ expression in the brain of mice bearing GBM (n = 5 per arm). (b) Summary plots of IFN-γ activity in CD4+ and CD8+ cells based on treatment modality (n = 5 per arm). (c) Flow cytometry plots demonstrating %parent populations of CD4+ and CD8+ TNF-α expression in the brain of mice bearing GBM (n = 5 per arm). (d) Summary plots of TNF-α activity in CD4+ and CD8+ cells based on treatment modality (n = 5 per arm). (*** $P < .001$, ** $P < .01$, * $P < .05$).

loaded therapeutic anti-PD-1. The former was given over three time points as described in previous studies[11], while mice treated with hydrogels were given a one-time injection in one of the following locations: intracranial at the site of the tumor, the left inguinal region or the left anterior cervical region. Due to spatial limitations with the murine intracranial compartment, a max dose of 200 ug in 6 ul of hydrogel was given.

However, all other mice were treated with a total of 600 ug of anti-PD-1 in 50 ul of hydrogel solution.

Gating strategies with markers for assessing CD4+ and CD8 + T cell activation were used to assess for the immunogenic potential of the hydrogel platform (Supplemental Figure 1a). Fluorescence minus one (FMO) for IFN-γ and TNF-α, immune activation markers that are upregulated in

activated immune cells such as CD4+ and CD8 + T lymphocytes (Supplemental Figure 1b), were utilized to indicate proportion of activated cell populations. Overall, there was greater IFN-γ and TNF-α activity from CD4+ and CD8 + T cells in the brains of mice treated with hydrogels in the inguinal and cervical regions. Notably, mice that were given hydrogels loaded with anti-PD-1 in the intracranial space showed comparable immunogenic changes to control mice without treatment. However, due to issues with limited volume in the intracranial space, these changes may be a reflection of the lower dose of anti-PD-1 (200 ug vs 600 ug) (Figure 3bd).

The overall trend of hydrogels demonstrating increased activation of CD4+ and CD8 + T lymphocytes is significant, with both IFN-γ and TNF-α showing increased representation in CD4+ and CD8+ populations in inguinal and cervical hydrogel models. In regard to IFN-γ specifically, there was an increase in percentage of CD4+ IFN-γ cells in the brain in mice treated with hydrogels in the deep cervical lymph node space compared to mice treated with systemically with i.p. anti-PD-1 ($P = .0007$) (Figure 3ab). Similarly, mice treated with hydrogels in the inguinal area also demonstrated increased expression of CD4+ IFN-γ cells compared to mice treated with i.p. anti-PD-1 ($P = .0430$). However, there was no significant difference in CD4+ IFN-γ expression in mice treated with hydrogels in either the inguinal or deep cervical lymph node regions (Figure 3ab). The expression of CD8+ IFN-γ-producing cells was highest in tumor-bearing mice treated with hydrogels loaded with anti-PD-1 in the deep cervical region compared to i.p. injected mice ($P = .0468$) and inguinal hydrogel mice ($P = .0229$). Interestingly, there was no significant difference in CD8+ IFN-γ-producing cell populations between mice treated via i.p. or by hydrogel in the inguinal region (Figure 3ab).

While TNF-α showed a similar overall trend for inguinal and cervical hydrogel models having increased activation of their lymphocyte compartments compared to i.p. treated mice, there was actually a trend toward more activation in the inguinal lymph node hydrogel system rather than with direct cervical lymph nodes. When examining CD4+ and CD8+ TNF-α binding cells, there was no significant difference between either hydrogel group ($P = .3134$ and $P = .6507$, respectively) (Figure 3 cd). However, there was a statistically significant difference between CD4+ and CD8+ TNF-α binding cells in the brain between i.p. treated and inguinal lymph node hydrogel mice ($P = .0316$ and $P = .0044$, respectively) (Figure 3 cd).

Survival efficacy is improved with localized sustained delivery to lymph nodes

To assess for the therapeutic efficacy of sustained and localized delivery of anti-PD-1 to lymph nodes, mice were implanted with GL261-Luc2 and selected for similar tumor burden via IVIS® before being randomly assorted to one of five arms: control (no treatment), i.p. systemic anti-PD-1 treatment (three 200 ug doses), anti-PD-1 loaded into a hydrogel in the intracranial space at the site of the tumor (one-time 200 ug dose), anti-PD-1 loaded into a hydrogel at the inguinal region (one-time 600 ug dose), and anti-PD-1 loaded into a hydrogel at the deep cervical lymph node region (one-time 600 ug dose) (Figure 4ab).

Overall, mice with hydrogels carrying anti-PD-1 at the inguinal and deep cervical lymph node regions exhibited improved overall survival compared to i.p. injected mice ($P = .0185$) (Figure 4c). There was no significant difference in therapeutic efficacy in mice treated with hydrogels in the
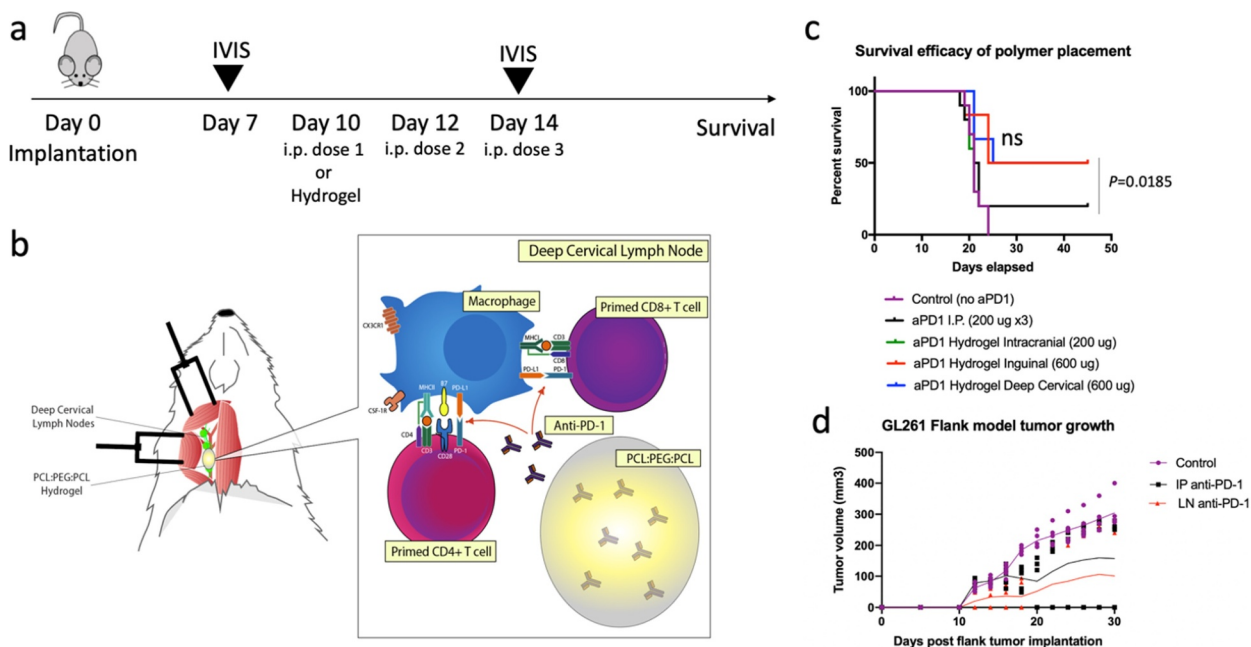
Figure 4. Survival efficacy of polymer placement involving anti-PD-1. (a) General timeline for dosing schedules for tumor-bearing mice implanted with hydrogel or treated systemically with anti-PD-1. (b) Pictured here are PCL:PEG:PCL hydrogels carrying anti-PD-1 for local delivery to cervical lymph nodes. The schematic demonstrates the proposed mechanism of how anti-PD-1 is impacting the T cell compartment. (c) Survival data of mice implanted with hydrogels vs systemic delivery of anti-PD-1 are demonstrated here, with mice implanted with hydrogels at the deep cervical lymph nodes demonstrating improved survival efficacy of systemic delivery (n = 10 per arm) ($P = .0185$).

inguinal or cervical region. Survival efficacy was similar between control and intracranial hydrogel mice, with the intracranial compartment limiting the dosage and thereby diminishing the comparative insight of this finding. Moreover, when examining the effect of hydrogel placement on local tumor growth in flank models involving GL261, there was a clear advantage in overall decreased rate of tumor growth in mice with hydrogel placement near the tumor. Intriguingly, despite establishing radiographic tumor burden through IVIS® on post-implantation day 7, three of the five mice that were implanted with hydrogel carrying anti-PD-1 did not develop measurable tumor burden (Figure 4d).

Polymer based delivery to lymph nodes results in increased IFN-γ in co-culture

To further examine the immunophenotypic changes that result from the long-term local presence of anti-PD-1 at the site of lymph nodes, isolated CD3 + T lymphocytes were harvested from the inguinal and deep cervical lymph nodes of mice treated with hydrogels at the inguinal and cervical site, respectively. Inguinal and cervical lymph nodes of mice without any treatment and mice with systemic anti-PD-1 therapy (i.p. injections) were used as comparative controls. These immune cells were co-cultured with dendritic cells and tumor cell lysate, with ELISA used to assess for production of IFN-γ.

In mice implanted with hydrogels at the inguinal region, there was no statistically significant difference between the expression of IFN-γ in CD3 + T lymphocytes between i.p. and hydrogel-treated arms (Figure 5a). However, there was a significant increase in IFN-γ expression in CD3+ lymphocytes from the deep cervical draining lymph nodes in mice that had hydrogels in the anterior cervical space compared to those that had i.p. therapy ($P = .0379$) (Figure 5b).

Discussion

The relatively recent advent of checkpoint blockade as an exciting therapeutic avenue has resulted in successes for multiple cancers, though there are important headways yet to be made in optimizing treatments. Currently, the main method of delivery for checkpoint blockade agents such as anti-PD-1 involves systemic delivery, which requires multiple infusions that may result in systemic toxicities. Our investigation demonstrates proof of principle that sustained and localized delivery of immunotherapeutic agents to lymph nodes is a viable therapeutic option in preclinical models, with resultant reversal of immunosuppression as demonstrated by increased IFN-γ and TNF-α activity in T lymphocytes as well as increased therapeutic efficacy compared to the current model of multiple systemic infusions (Figure 4). Moreover, we demonstrate in our preclinical model that there is also less delivery of anti-PD-1 to other organs with hydrogel-based therapy, with the majority of anti-PD-1 being released to the local lymph node and the site of tumor (Figures 1 and Figure 2). Additionally, there was unexpected insight into how anti-PD-1 traverses the blood–brain barrier (BBB) and localizes to the brain specifically in mice with tumors, otherwise exhibiting a marginal presence in the healthy brain (Figures 1 and Figure 2). It is unclear at this time, however, if the antibody is being bound to immune cells and trafficking to the brain, if the free antibody itself traverses the compromised blood–brain barrier, or if a combination of both events occurs.

Recently, there has been much interest in targeting GBM locally in the intracranial compartment with both chemotherapy and immunotherapy. However, our study offers an alternative target that prescribes local therapy to lymph nodes – in this case the deep cervical and inguinal lymph nodes. Interestingly, while there was a greater trend toward reversing immunosuppression with treatment of the deep cervical lymph
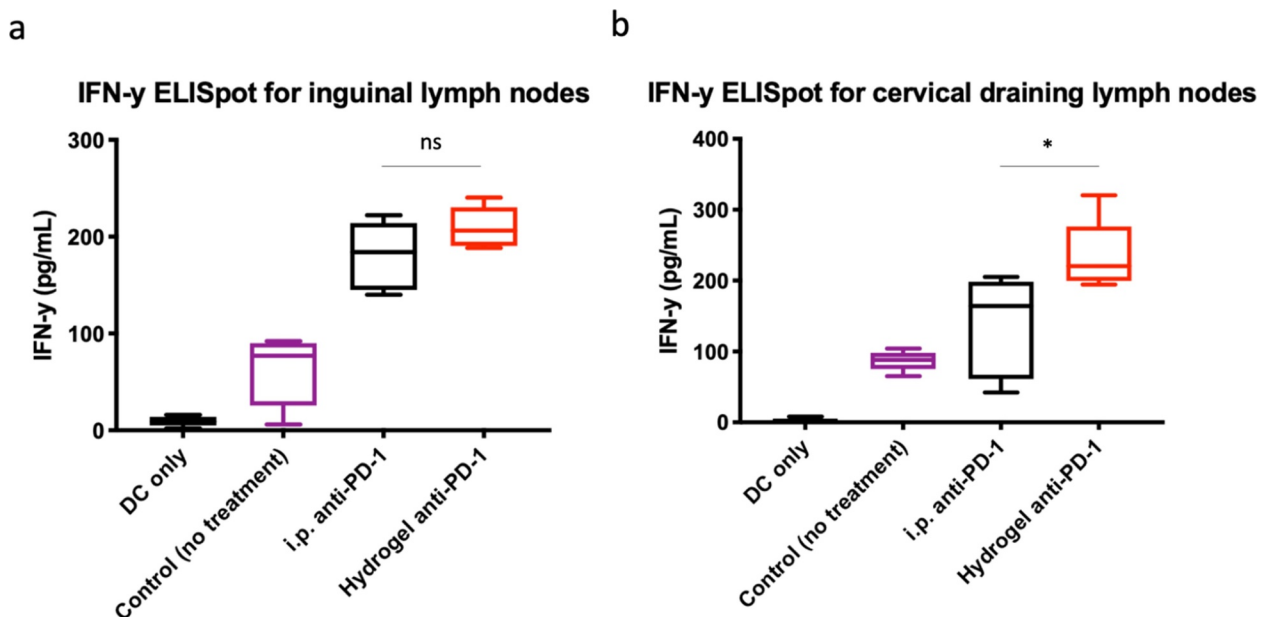
Figure 5. *In vitro* co-culture assay for IFN-γ expression with ELISA. (a) T cells were isolated via FACS microfluidic sorting from mouse cervical and inguinal lymph nodes that were treated with anti-PD-1 monotherapy (intraperitoneal vs polymer placement) and co-cultured with GL261 tumor cell lysate and CD11c+ dendritic cells and plotted for concentration of IFN-γ in supernatant of co-culture wells (n = 6 per arm) (* $P < .05$).

nodes when looking at IFN-γ expression alone, the therapeutic efficacy of targeting either the inguinal or deep cervical lymph nodes was similar in our murine model. This may be in part accounted by other activating cytokines such as TNF-α that showed trends toward increased activation of lymphocytes in inguinal lymph nodes compared to cervical lymph nodes. In either case, however, placement of anti-PD-1 releasing hydrogels in inguinal and cervical lymph nodes demonstrates increased activation of CD4+ and CD8+ populations compared to mice injected systemically with anti-PD-1. While there are many more avenues to explore regarding local lymph node delivery, our data demonstrate proof of principle of targeting lymph nodes with sustained delivery as a viable target for reactivating immune cells.

Finally, our observations regarding accumulation of anti-PD-1 in the brain selectively over other non-lymphoid tissues in the context of tumors could be explained by prior studies in immune cell homeostasis and trafficking. In previous studies, we have observed T cell activation and expansion against tumor-derived antigens in the draining lymph nodes over many days following adoptive transfer of tumor-specific T cells in murine models of glioma (including on day 5).[11,21,22] Because these anti-tumor T cells are concentrated in the lymph nodes and exposed to local anti-PD-1 during activation, we propose that upon infiltrating the tumor they allow accumulation of anti-PD-1 in the brain gradually. On the other hand, we suspect that i.p. treated mice do not have adequate binding of anti-PD-1 as they would be binding to more diffuse circulating tumor-reactive T cells; this is further challenged by the relatively short half-life of circulating anti-PD-1 (22.3 hours)[23]. As mentioned before, there are likely differences in immune cell populations and activating cytokines between inguinal and cervical lymph nodes that were not able to be fully explored in the scope of this study.

Several studies have supported the concept of targeted therapies of lymph nodes. For instance, tumor-specific CD8 + T cells have long since been understood as undergoing activation in the tumor-draining lymph nodes, with the potential to differentiate into anti-tumor effector phenotypes occurring at these robust immune sites[24]. Moreover, it has already been well established that tumor-specific T cell responses are initiated in lymph nodes where antigen presentation is occurring[12]. In both mouse models and humans, CD103+ (mouse) and CD141+ (human) migratory dendritic cells were found to carry tumor antigens to lymph nodes and cross-present them to CD8 + T lymphocytes.[13,14] Moreover, this is all in light of the unforgiving nature of the physical tumor microenvironment of GBM – with its hypoxic and necrotic features as well as tumorigenic stromal neighbors – that presents an ongoing challenge with local immunotherapy at the site of the tumor[8]. As such, the slightly less immunosuppressive environment of lymph nodes offers a much more enviable target for reversing immunosuppression[3].

Previous studies have suggested that anti-tumor T cell responses can be promoted more robustly in lymph nodes distal from brain tumors, but only in the context of local injection of tumor-vaccines, which overcomes the hurdle of antigen drainage to distal lymph nodes[25]. In our current study, it may be possible that inguinal-injected hydrogel acts as a depot to deliver anti-PD-1 to lymphocytes en route to the site of anti-tumor priming in more proximal tumor draining lymph nodes; this might also explain the lower proportion of lymph node T cell activation in the inguinal lymph nodes (Figure 5). However, there are also studies that suggest that inguinal lymph nodes may communicate with spinal cerebrospinal fluid (CSF) and also act as surrogate tumor-draining lymph nodes to the CNS compartment, which may in turn that may have antigen presentation[26]. Investigating the nature of CD4 and CD8 activation following anti-PD-1 at distal and proximal lymph nodes is warranted to further understand their respective roles in the rejuvenation of an anti-tumor response.

Finally, while we used anti-PD-1 as a proof of principle for delivering sustained and localized immunotherapy, the potential for using a depot form for delivering other immunomodulating therapies such as stimulator of interferon genes (STING) agonists to target myeloid cells at the level of the lymph node also holds potential. Limitations of this study included lack of side effect profiles to determine whether there was mitigation of irAEs with localized therapy to lymph nodes of interest, though this was also a reflection of the limits of our current mouse model. Additionally, the dosage discrepancy between intracranial (limited by the enclosed compartment of the mouse cranium) and lymph node anti-PD-1 hydrogel delivery makes it difficult for meaningful comparison. Furthermore, to test the robustness of local and sustained immunotherapeutic delivery to lymph nodes, additional agents that target different immune compartments within lymph nodes would have offered more detailed information. Finally, while this study showed proof of principle for targeting lymph nodes using sustained release of immunotherapy as a viable treatment avenue, more in-depth analysis of the different cell populations and their interactions involving immunosuppressive and activating cytokines at the level of different lymph nodes should be explored in future studies. Future directions would likely include combinatorial immunotherapy strategies that target the tumor draining lymph nodes for neoadjuvant access to the immune compartment with accompanying surgical resection, chemotherapy, and radiation.

ORCID

Michael Lim http://orcid.org/0000-0003-0523-3076

References

1. Goldberg MV, Maris CH, Hipkiss EL, Flies AS, Zhen L, Tuder RM, Grosso JF, Harris TJ, Getnet D, Whartenby KA, et al.. Role of PD-1 and its ligand, B7-H1, in early fate decisions of CD8 T cells. Blood. 2007;110(1):186–192. doi:10.1182/blood-2006-12-062422.

2. Tsushima F, Yao S, Shin T, Flies A, Flies S, Xu H, Tamada K, Pardoll DM, Chen L. Interaction between B7-H1 and PD-1 determines initiation and reversal of T-cell anergy. Blood. 2007;110(1):180–185. doi:10.1182/blood-2006-11-060087.

3. Topalian SL, Taube JM, Pardoll DM. Neoadjuvant checkpoint blockade for cancer immunotherapy. Science . 2020;367(80):6477. doi:10.1126/science.aax0182.

4. Blackburn SD, Crawford A, Shin H, Polley A, Freeman GJ, Wherry EJ. Tissue-specific differences in PD-1 and PD-L1 expression during chronic viral infection: implications for CD8 T-cell exhaustion. J Virol. 2010;84(4):2078–2089. doi:10.1128/jvi.01579-09.

5. Khan BT. Pembrolizumab for patients with advanced melanoma. Lancet Oncol. 2015;16(6):e264. doi:10.1016/S1470-2045(15)70193-2.

6. Reck M, Rodriguez-Abreu D, Robinson AG, Hui R, Csőszi T, Fülöp A, Gottfried M, Peled N, Tafreshi A, Cuffe S, et al.. Pembrolizumab versus chemotherapy for PD-L1-positive non-small-cell lung cancer. N Engl J Med. 2016;375(19):1823–1833. doi:10.1056/NEJMoa1606774.

7. Larkin J, Chiarion-Sileni V, Gonzalez R, Grob -J-J, Rutkowski P, Lao CD, Cowey CL, Schadendorf D, Wagstaff J, Dummer R, et al.. Five-year survival with combined nivolumab and ipilimumab in advanced melanoma. N Engl J Med. 2019;381(16):1535–1546. doi:10.1056/NEJMoa1910836.

8. Jackson CM, Choi J, Lim M. Mechanisms of immunotherapy resistance: lessons from glioblastoma. Nat Immunol. 2019;20(9):1100–1109. doi:10.1038/s41590-019-0433-y.

9. Woroniecka K, Chongsathidkiet P, Rhodin K, Kemeny H, Dechant C, Farber SH, Elsamadicy AA, Cui X, Koyama S, Jackson C, et al.. T-cell exhaustion signatures vary with tumor type and are severe in glioblastoma. Clin Cancer Res. 2018;24(17):4175–4186. doi:10.1158/1078-0432.CCR-17-1846.

10. Almutairi AR, McBride A, Slack M, Erstad BL, Abraham I. Potential immune-related adverse events associated with monotherapy and combination therapy of ipilimumab, nivolumab, and pembrolizumab for advanced melanoma: a systematic review and meta-analysis. Front Oncol. 2020:10. doi:10.3389/fonc.2020.00091.

11. Kim JE, Patel MA, Mangraviti A, Kim ES, Theodros D, Velarde E, Liu A, Sankey EW, Tam A, Xu H, et al.. Combination therapy with anti-PD-1, anti-TIM-3, and focal radiation results in regression of murine gliomas. Clin Cancer Res. 2017;23(1):124–136. doi:10.1158/1078-0432.CCR-15-1535.

12. Rotman J, Koster BD, Jordanova ES, Heeren AM, de Gruijl TD. Unlocking the therapeutic potential of primary tumor-draining lymph nodes. Cancer Immunol Immunother. 2019;68(10):1681–1688. doi:10.1007/s00262-019-02330-y.

13. Roberts EW, Broz ML, Binnewies M, Headley MB, Nelson AE, Wolf DM, Kaisho T, Bogunovic D, Bhardwaj N, Krummel MF, et al..

14. Critical role for CD103 + /CD141 + dendritic cells bearing CCR7 for tumor antigen trafficking and priming of T cell immunity in melanoma. Cancer Cell. 2016;30(2):324–336. doi:10.1016/j.ccell.2016.06.003.

14. Salmon H, Idoyaga J, Rahman A, Leboeuf M, Remark R, Jordan S, Casanova-Acebes M, Khudoynazarova M, Agudo J, Tung N, et al.. Expansion and activation of CD103 + dendritic cell progenitors at the tumor site enhances tumor responses to therapeutic PD-L1 and BRAF inhibition. Immunity. 2016;44(4):924–938. doi:10.1016/j.immuni.2016.03.012.

15. Fransen MF, Schoonderwoerd M, Knopf P, Camps MGM, Hawinkels LJAC, Kneilling M, van Hall T, Ossendorp F. Tumor-draining lymph nodes are pivotal in PD-1/PD-L1 checkpoint therapy. JCI Insight. 2018;3(23):23. doi:10.1172/jci.insight.124507.

16. Strauss L, Mahmoud MAA, Weaver JD, Tijaro-Ovalle NM, Christofides A, Wang Q, Pal R, Yuan M, Asara J, Patsoukis N, et al.. Targeted deletion of PD-1 in myeloid cells induces antitumor immunity. Sci Immunol. 2020;5(43):43. doi:10.1126/sciimmunol.aay1863.

17. Zeng J, See AP, Phallen J, Jackson CM, Belcaid Z, Ruzevick J, Durham N, Meyer C, Harris TJ, Albesiano E, et al.. Anti-PD-1 blockade and stereotactic radiation produce long-term survival in mice with intracranial gliomas. Int J Radiat Oncol. 2013;86(2):343–349. doi:10.1016/j.ijrobp.2012.12.025.

18. Hirano F, Kaneko K, Tamura H, et al.. Blockade of B7-H1 and PD-1 by monoclonal antibodies potentiates cancer therapeutic immunity. 2005.

19. Brechbiel MW, Gansow OA. Synthesis of C-functionalized trans-cyclohexyldiethylenetriaminepenta-acetic acids for labelling of monoclonal antibodies with the bismuth-212 α-particle emitter. J Chem Soc Perkin Trans. 1992;1(9):1173–1178. doi:10.1039/P19920001173.

20. Chongsathidkiet P, Jackson C, Koyama S, Loebel F, Cui X, Farber SH, Woroniecka K, Elsamadicy AA, Dechant CA, Kemeny HR, et al.. Sequestration of T cells in bone marrow in the setting of glioblastoma and other intracranial tumors. Nat Med. 2018;24(9):1459–1468. doi:10.1038/s41591-018-0135-2.

21. Jackson CM, Kochel CM, Nirschl CJ, Durham NM, Ruzevick J, Alme A, Francica BJ, Elias J, Daniels A, Dubensky TW, et al.. Systemic tolerance mediated by melanoma brain tumors is reversible by radiotherapy and vaccination. Clin Cancer Res. 2016;22(5):1161–1172. doi:10.1158/1078-0432.CCR-15-1516.

22. Garzon-Muvdi T, Theodros D, Luksik AS, Maxwell R, Kim E, Jackson CM, Belcaid Z, Ganguly S, Tyler B, Brem H, et al.. Dendritic cell activation enhances anti-PD-1 mediated immunotherapy against glioblastoma. Oncotarget. 2018;9(29):20681–20697. doi:10.18632/oncotarget.25061.

23. Zalba S, Contreras-Sandoval AM, Martisova E, Debets R, Smerdou C, Garrido MJ. Quantification of pharmacokinetic profiles of pd-1/pd-l1 antibodies by validated elisas. Pharmaceutics. 2020;12(6):1–16. doi:10.3390/pharmaceutics12060595.

24. Prokhnevska N, Cardenas M, Jansen C, et al.. Tumor-specific CD8 T cell activation in draining lymph nodes supports the anti-tumor CD8 T cell response. J Immunol. 2020;204(1Supplement).

25. Ohlfest JR, Andersen BM, Litterman AJ, Xia J, Pennell CA, Swier LE, Salazar AM, Olin MR. Vaccine injection site matters: qualitative and quantitative defects in CD8 T cells primed as a function of proximity to the tumor in a murine glioma model. J Immunol. 2013;190(2):613–620. doi:10.4049/jimmunol.1201557.

26. Ma Q, Schlegel F, Bachmann SB, et al.. Lymphatic outflow of cerebrospinal fluid is reduced in glioma. Sci Rep. 2019;9(1):1–10. doi:10.1038/s41598-019-51373-9.